

Gadolinium accumulation using Gd-DTPA-incorporated Calcium Phosphate Nanoparticles for Gd-neutron capture therapy

N. Dewi^{1,5}, P. Mi^{2,3}, H. Yanagie^{1,4,5}, Y. Sakurai⁴, H. Cabral², N. Nishiyama³, K. Kataoka^{2,6}, Y. Sakurai⁷, H. Tanaka⁷, M. Suzuki⁷, S. Masunaga⁷, K. Ono⁷, Minoru Ono^{4,8}, Jun Nakajima^{4,9}, and H. Takahashi^{1,4}

¹Dept of Nuclear Engineering & Management, Univ of Tokyo, ²Bioengineering Dept, Univ of Tokyo, ³Polymer chemistry division, Chemical Resource Laboratory, Tokyo Institute of Technology, ⁴Cooperative Unit of Medicine & Engineering, Univ of Tokyo Hospital, ⁵Dept of Innovative Cancer Therapeutics, Meiji Pharmaceutical University, ⁶Materials Engineering Dept, The University of Tokyo, ⁷Research Reactor Institute, Kyoto University, ⁸Dept of Cardiac Surgery, The University of Tokyo Hospital, ⁹Dept of Thoracic Surgery, The University of Tokyo Hospital

INTRODUCTION: Gadolinium-157 has been getting attention as an attractive agent for neutron capture therapy (NCT) because of its high thermal neutron cross section (255 000 barns), which is the highest among all stable elements. However, gadolinium neutron capture reaction (Gd-NCR) results in release of gamma rays, which reduce the localization effect of the treatment, increasing the possible additional effect if Gd-157 is accumulated to a bulk tumor cluster [1].

We synthesized Gd-DTPA-incorporated Calcium Phosphate (Gd-DTPA/CaP) nanoparticles with two-step preparation method by self-assembly poly(ethylene glycol)-b-poly(aspartic acid) block copolymer, Gd-DTPA, and CaP in aqueous solution, followed with hydrothermal treatment. Evaluation of possible apoptosis by detecting the DNA fragmentation following GdNCT treatment has shown that the number of cells killed after treatment was observed to be similar for single and multiple injection groups of Gd-DTPA/CaP nanoparticles, while non-treated group shows normal histology with clear cytoplasm and nucleus [3].

In this work, we evaluated the tumor accumulation of Gd atoms for single and multiple injections using Gd-DTPA/CaP nanoparticles.

EXPERIMENTS: We carried out the biodistribution experiments of in vivo quantitative analysis, each for single and multiple injections of Gd-DTPA/CaP nanoparticles. To confirm the pharmacokinetics of Gd-DTPA/CaP nanomicelles for 0.2 mL single injection, tumor, blood, and other organ samples were harvested at 12 and 24 hr following nanoparticles administration. Three times injections of Gd-DTPA/CaP nanomicelles with 10 hr interval were then carried out in order to achieve higher gadolinium accumulation in tumor site. Samples from both experiments were analyzed using ICP-MS.

RESULTS: Quantitative analysis from ICP-MS measurement results of gadolinium accumulation in tumor and several mice organs were shown in Table 1. We could achieve the tumor-to-blood (T/B) ratio of around 2.4 at 24 hr after Gd-DTPA/CaP nanoparticles injection.

Table 1. Gd accumulation in tumor and several organs of tumor bearing mice after single injection of Gd-DTPA/CaP nanoparticles

	Gd concentration ($\mu\text{g/g}$ or mL)	
	12hr	24hr
Tumor	5.85 \pm 0.64	8.03 \pm 0.82
Blood	14.55 \pm 0.50	3.29 \pm 0.40
Liver	10.71 \pm 0.17	16.71 \pm 0.60
Spleen	7.08 \pm 0.41	10.03 \pm 0.30
Kidney	2.66 \pm 0.24	2.13 \pm 0.06
Brain	0.16 \pm 0.01	0.04 \pm 0.01

Higher gadolinium accumulation in tumor site was successfully achieved for multiple injections of Gd-DTPA/CaP nanoparticles as shown in Figure 1. Gadolinium concentration reached the amount of more than three times higher compared to those at 10 hr after the first injection. Significant increase in gadolinium concentration in blood plasma was also observed at 30hr after first injection. This result indicates the prolonged blood circulation of Gd-DTPA/CaP nanoparticles.

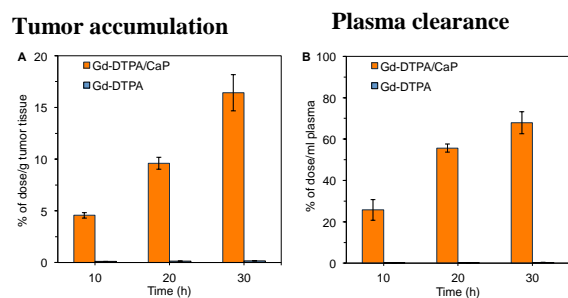


Figure 1. Gadolinium biodistribution for multiple injections. Higher gadolinium accumulation in tumor site was achieved significantly after three times injection. More than 60% of injected dose of gadolinium was still observed in plasma indicating the prolonged blood circulation of Gd-DTPA/CaP nanoparticles.

REFERENCES:

- [1] Dewi N et al., Biomed & Pharmacother (2013) **67**:451-7.
- [2] Mi P, et al.: [ACS Nano](#) (2015) **23**;9(6):5913-21.
- [3] Dewi N et al., J Can.Res.Clin.Oncol. (2016) **142**(4):767-75.

CO7-2 A Fundamental Experiment for the Measure Against the Activation of the Irradiation-room Concrete at BNCT Facility (III)

T. Takata, Y. Sakurai, K. Kimura¹, H. Tanaka, K. Takamiya

Research Reactor Institute, Kyoto University
¹Fujita Corporation

INTRODUCTION: At present time, the research and development of accelerator-based neutron sources for boron neutron capture therapy (BNCT) are underway by several research groups around the world, with Cyclotron-based BNCT Epi-thermal Neutron Source (C-BENS) in the lead [1]. In near future, BNCT using the accelerator-based neutron sources may be carried out at several places in the world. Compared to irradiation facilities for X-ray and charged-particle radiation therapy, the neutron yield is much larger at BNCT facility. Thus, the activation of concrete, which is a main structure material of the irradiation facility, becomes an issue from the viewpoints of radiation exposure of medical workers, the decommissioning of the facility, etc.. This research is intended to perform the characteristic estimation of the materials for activation reduction and to confirm its usability at BNCT facility. In 2016, characteristic estimation of a neutron shielding material covering concrete wall surfaces was performed by using an Am-Be neutron source in the same manner in 2014 and 2015 [2], because Kyoto University Reactor (KUR) was not operated.

METHODS: A characteristic estimation was performed for the resin-based shielding materials containing B₄C with different particle sizes. The small-size particles were used in the sample A, in which the B₄C can be considered to be distributed homogeneously in the resin. On the other hands, the particles with a submillimeter diameter were used in the sample B, in which the B₄C was localized in the particles and thus considered to be distributed sparsely in the resin. These samples were prepared to have the almost same B₄C concentration level as a whole volume average. Four resin sheets of 10-cm side, 10-cm long and 4-mm thickness were stacked on the concrete surface. The shielding performance against the Am-Be neutron source was estimated by activation method of indium foils placed between the stacked resin layers. The characteristic for fast neutron shielding was estimated by the change in the $^{115}\text{In}(n,n')^{115\text{m}}\text{In}$ reaction rate, and the characteristic for thermal neutron generation was estimated by the change in the $^{115}\text{In}(n,\gamma)^{116\text{m}}\text{In}$ reaction rate.

RESULTS: Figures 1 and 2 show the reaction rates for the $^{115}\text{In}(n,n')^{115\text{m}}\text{In}$ and $^{115}\text{In}(n,\gamma)^{116\text{m}}\text{In}$ reactions, respectively, as a function of the neutron-shield thickness of the sample A and B. From the comparison of the changes in the $^{115}\text{In}(n,n')^{115\text{m}}\text{In}$ reaction rate, the shielding ability for fast neutrons was found to be almost same between the sample A and B. From the comparison of the changes in the $^{115}\text{In}(n,\gamma)^{116\text{m}}\text{In}$ reaction rate, the generation of ther-

mal neutrons was found to be slightly larger in the sample B compared to the sample A.

CONCLUSION: Toward the restart of KUR operation, the estimations for the important characteristics of the shielding materials as well as the low-activation concrete materials are planned, such as the shielding effect for neutrons and gamma rays, the generation of the secondary gamma rays, etc., using Heavy Water Neutron Irradiation Facility [3]. Also, the neutron activation analysis for these materials and its basic ingredients using Pneumatic Tubes is planned to estimate the activation characteristics from short to long time range.

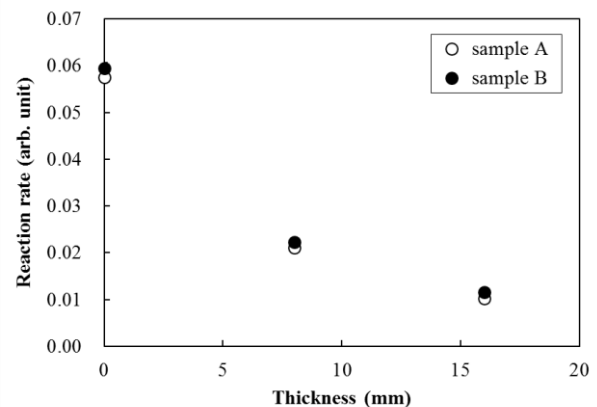


Fig. 1. $^{115}\text{In}(n,n')^{115\text{m}}\text{In}$ reaction rate as a function of the shield thickness.

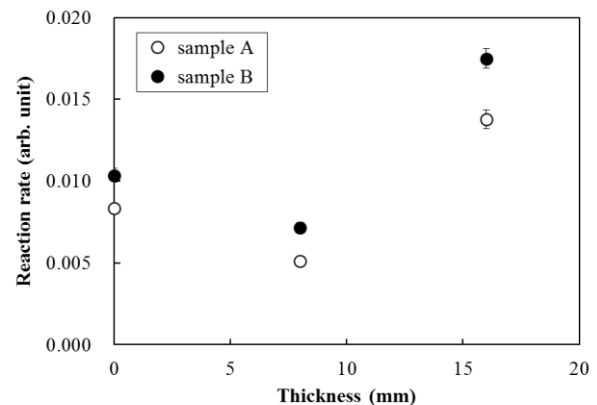


Fig. 2. $^{115}\text{In}(n,\gamma)^{116\text{m}}\text{In}$ reaction rate as a function of the shield thickness.

REFERENCES:

- [1] H. Tanaka *et al.*, Nucl. Instr. Meth. B **267** (2009) 1970-1977.
- [2] Y. Sakurai, T. Takata *et al.*, KURRI Progress Report 2015 (2016) 97.
- [3] Y. Sakurai *et al.*, Nucl. Instr. Meth. A **453** (2000) 569-596.